NASA/TM—2001-211117 ARL–TR–1314

Effect of Speed (Centrifugal Load) on Gear Crack Propagation Direction

David G. Lewicki
U.S. Army Research Laboratory, Glenn Research Center, Cleveland, Ohio

August 2001

The NASA STI Program Office . . . in Profile

Since its founding, NASA has been dedicated to the advancement of aeronautics and space science. The NASA Scientific and Technical Information (STI) Program Office plays a key part in helping NASA maintain this important role.

The NASA STI Program Office is operated by Langley Research Center, the Lead Center for NASA's scientific and technical information. The NASA STI Program Office provides access to the NASA STI Database, the largest collection of aeronautical and space science STI in the world. The Program Office is also NASA's institutional mechanism for disseminating the results of its research and development activities. These results are published by NASA in the NASA STI Report Series, which includes the following report types:

- TECHNICAL PUBLICATION. Reports of completed research or a major significant phase of research that present the results of NASA programs and include extensive data or theoretical analysis. Includes compilations of significant scientific and technical data and information deemed to be of continuing reference value. NASA's counterpart of peer-reviewed formal professional papers but has less stringent limitations on manuscript length and extent of graphic presentations.

- TECHNICAL MEMORANDUM. Scientific and technical findings that are preliminary or of specialized interest, e.g., quick release reports, working papers, and bibliographies that contain minimal annotation. Does not contain extensive analysis.

- CONTRACTOR REPORT. Scientific and technical findings by NASA-sponsored contractors and grantees.

- CONFERENCE PUBLICATION. Collected papers from scientific and technical conferences, symposia, seminars, or other meetings sponsored or cosponsored by NASA.

- SPECIAL PUBLICATION. Scientific, technical, or historical information from NASA programs, projects, and missions, often concerned with subjects having substantial public interest.

- TECHNICAL TRANSLATION. English-language translations of foreign scientific and technical material pertinent to NASA's mission.

Specialized services that complement the STI Program Office's diverse offerings include creating custom thesauri, building customized data bases, organizing and publishing research results . . . even providing videos.

For more information about the NASA STI Program Office, see the following:

- Access the NASA STI Program Home Page at ***http://www.sti.nasa.gov***

- E-mail your question via the Internet to help@sti.nasa.gov

- Fax your question to the NASA Access Help Desk at 301–621–0134

- Telephone the NASA Access Help Desk at 301–621–0390

- Write to:
  NASA Access Help Desk
  NASA Center for AeroSpace Information
  7121 Standard Drive
  Hanover, MD 21076

NASA/TM—2001-211117

ARL–TR–1314

Effect of Speed (Centrifugal Load) on Gear Crack Propagation Direction

David G. Lewicki
U.S. Army Research Laboratory, Glenn Research Center, Cleveland, Ohio

Prepared for the
International Conference on Motion and Power Transmissions
sponsored by the Japan Society of Mechanical Engineers
Fukuoka, Japan, November 15–17, 2001

National Aeronautics and
Space Administration

Glenn Research Center

August 2001

Available from

NASA Center for Aerospace Information
7121 Standard Drive
Hanover, MD 21076

National Technical Information Service
5285 Port Royal Road
Springfield, VA 22100

Available electronically at http://gltrs.grc.nasa.gov/GLTRS

EFFECT OF SPEED (CENTRIFUGAL LOAD) ON GEAR CRACK PROPAGATION DIRECTION

David G. Lewicki
U.S. Army Research Laboratory
National Aeronautics and Space Administration
Glenn Research Center
Cleveland, Ohio 44135

Keywords: Crack Propagation , Fracture Mechanics, Centrifugal Force, Finite Element Method

ABSTRACT

The effect of rotational speed (centrifugal force) on gear crack propagation direction was explored. Gears were analyzed using finite element analysis and linear elastic fracture mechanics. The analysis was validated with crack propagation experiments performed in a spur gear fatigue rig. The effects of speed, rim thickness, and initial crack location on gear crack propagation direction were investigated. Crack paths from the finite element method correlated well with those deduced from gear experiments. For the test gear with a backup ratio (rim thickness divided by tooth height) of m_b=0.5, cracks initiating in the tooth fillet propagated to rim fractures when run at a speed of 10,000 rpm and became tooth fractures for speeds slower than 10,000 rpm for both the experiments and analysis. From additional analysis, speed had little effect on crack propagation direction except when initial crack locations were near the tooth/rim fracture transition point for a given backup ratio. When at that point, higher speeds tended to promote rim fracture while lower speeds (or neglecting centrifugal force) produced tooth fractures.

INTRODUCTION

Effective gear designs balance strength, durability, reliability, size, weight, and cost. However, unexpected gear failures may occur even with adequate gear tooth design [1]. In order to design an extremely safe system, the designer must ask and address the question "what happens when a failure occurs". With regard to gear tooth bending fatigue, tooth or rim fractures may occur. For aircraft, a crack which propagates through a rim would be catastrophic, leading to disengagement of a rotor or propeller, loss of an aircraft, and possible fatalities [2]. This failure mode should be avoided. A crack which propagates through a tooth itself may or may not be catastrophic, depending on the design and operating conditions. Also, early warning of this failure mode may be possible due to advances in modern diagnostic systems.

Fracture mechanics has developed into a useful discipline for predicting strength and life of cracked structures. Linear elastic fracture mechanics applied to gear teeth has become increasingly popular. The stress intensity factors are the key parameters to estimate the characteristics of a crack. Analytical methods (such as weight function techniques) as well as numerical methods have been used to estimate gear tooth stress intensity factors [3-4]. Based on stress intensity factors, fatigue crack growth and gear life predictions have been investigated [5-6]. In addition, gear crack trajectory predictions have been addressed in a few studies [7-10]. In high speed components, centrifugal force can significantly contribute to the applied loading of the structure. This effect on crack propagation has been investigated for turbine blades [11] but has not been looked at with respect to gears.

The objective of the current study is to determine the effect of centrifugal force on gear crack propagation. The goal is to prevent catastrophic rim fracture failure modes when considering gear tooth bending fatigue. Analysis was performed using the finite element method with principles of linear elastic fracture mechanics. Crack propagation paths were predicted for a variety of gear tooth and rim configurations. Experiments were performed in a gear fatigue apparatus to validate crack predictions. The effects of speed (centrifugal force), rim thickness, and initial crack location were considered. Crack trajectories are presented for the variety of cases studied indicating gear tooth or gear rim fracture modes.

ANALYSIS

Basic gear tooth geometry data was input to a tooth coordinate generation computer program. The tooth coordinate generator program used the method of [12] to determine the tooth coordinates. The output was tooth coordinate and rim coordinate data which defined a single-tooth sector of a gear. This output was used by a commercially available pre- and post-processing finite element analysis software package [13]. This package created the finite element mesh of the complete gear. The mesh was then imported to the FRANC (FRacture ANalysis Code) computer program.

FRANC is a general purpose finite element code for the static analysis of cracked structures [14]. The program is designed for two-dimensional problems, uses principles of linear elastic fracture mechanics, and is capable of analyzing plane strain, plane stress, or axi-symmetric problems. Eight-node quadrilateral or six-node triangular elements can be used. Point forces can be applied at nodes to simulate gear tooth loading. Also, body forces due to angular rotation can be used to account for centrifugal force speed effects. The deflections, stresses, and stress intensity factors from the point forces and body forces can then be added together using superposition.

Among the variety of capabilities, a unique feature of the program is the ability to model a crack in a structure. The program uses a method called "delete and fill" to accomplish this. To illustrate, consider a finite element mesh of an uncracked structure. The user would first define an initial crack by identifying the node of the crack mouth and coordinates of the crack tip (Fig. 1a). FRANC would then delete the elements in the vicinity of the crack tip, insert a rosette of quarter-point, six-node triangular elements around the crack tip to model the inverse square-root stress singularity, then fill the remaining area between the rosette and original mesh with conventional six-node triangular elements (Fig. 1b). The user would then run the finite element equation solver to determine nodal displacements, forces, stresses, and strains. Mode I and mode II stress intensity factors, K_I and K_{II}, respectively, can be calculated using a variety of methods. (Mode I loading refers to loads applied normal to the crack plane which tend to open the crack. Mode II refers to in-plane shear loading. In addition, the crack propagation angle is a function of K_{II} / K_I.) The stress intensity factors quantify the state of stress in the region near the crack tip. In the program, the stress intensity factors can also be used to predict the crack propagation trajectory angles, again using a variety of methods.

A further unique feature of FRANC is the automatic crack propagation capability. After an initial crack is inserted in a mesh, the program simulates crack propagation as a number of straight line segments. For each segment (or step), the program solves the

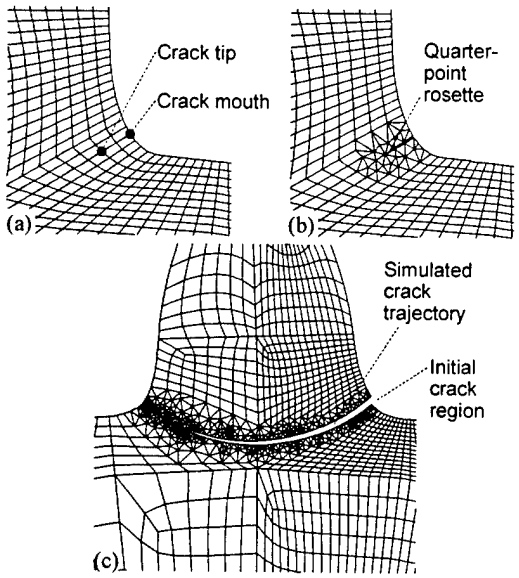

Fig. 1. Crack modeling scheme using finite element method. (a) user-defined initial crack, (b) final mesh of initial crack, (c) predicted crack propagation path.

finite element equations, calculates the stress intensity factors, and calculates the crack propagation angle. The program then places the new crack tip at the calculated angle and at a user-defined crack increment length. The model is then re-meshed using the "delete and fill" method described above. The procedure is repeated a number of times as specified by the user. Fig. 1c shows the predicted crack propagation path of a gear tooth. In this example, the predicted crack trajectory was after 29 steps, i.e., the crack trajectory was approximated by 29 line segments.

A typical finite element gear model used in the current study is shown in Fig. 2. The mesh shown is for an uncracked gear. The gear design is the baseline used in the current study. The design parameters are: 28 teeth, 3.175-mm module, 44.45-mm pitch radius, 20° pressure angle, and a 6.35-mm face width. The model had 2255 plane stress, 8-node, quadrilateral elements and 7122 nodes. For improved accuracy, the mesh was refined in the upper portion of the model (this is the region where cracks will be inserted). The tooth load was placed at the highest point of single tooth contact (HPSTC), normal to the surface. Although the tooth load changes in magnitude and direction in actual gear operations, a static analysis with the load at the HPSTC has given accurate results with respect to crack propagation analysis [9]. Four hub nodes at the gear inner diameter were fixed to ground to constrain the model. The material used was steel. In addition, slots were incorporated in the model to vary the rim thickness. The model shown has a backup ratio, m_b=1.0. The backup ratio is defined as the rim thickness, b, divided by the tooth height, h (Fig. 3). As stated before, crack propagation angles are determined from the calculated stress intensity factors. In the current study, the stress intensity factors were determined from the finite element method nodal displacements and forces using the J-integral method [15]. In addition, the crack propagation angles were determined from the stress intensity factors using the maximum tangential stress theory [16].

EXPERIMENTS

Crack propagation experiments were performed in the NASA Glenn Spur Gear Fatigue Rig (Fig. 4). The test stand operated on a torque-regenerative principle in which torque was circulated in a loop of test gears and slave gears. Oil pressure was supplied to load vanes in one slave gear which displaced the gear with respect to its

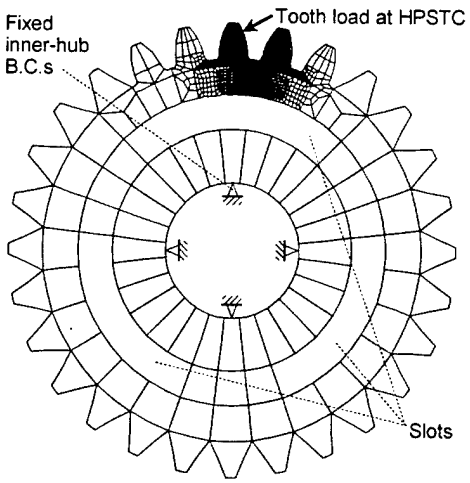

Fig. 2. Typical finite element model of an uncracked gear; 28 teeth, 3.175-mm module, 44.45-mm pitch radius, 20° pressure angle, m_b=1.0.

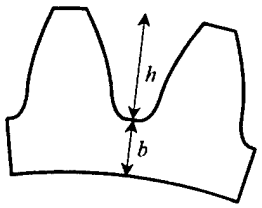

Fig. 3. Definition of terms backup ratio, $m_b=b/h$.

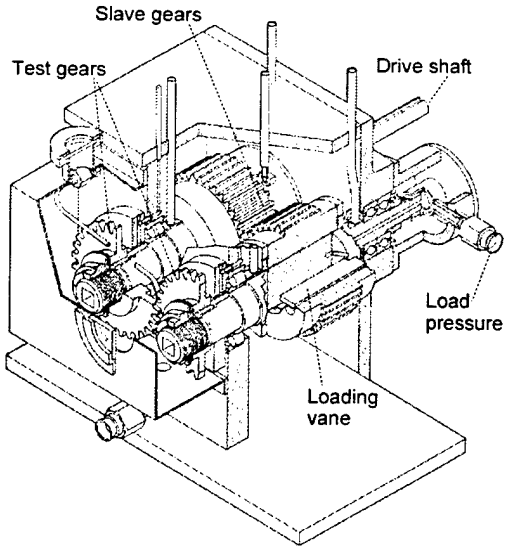

Fig. 4. NASA Glenn spur gear fatigue rig.

shaft. This produced a torque on the test gears, slave gears, and connecting shafts proportional to the amount of applied oil pressure. An 18.6-kW, variable-speed motor provided speed to the drive shaft using a belt and pulley. Note that in a torque-regenerative system, the required input drive power needs only to overcome the losses in the system.

Separate lubrication systems were provided for the tests gears and the main gearbox. The test gears were lubricated using a single oil jet at the in-to-mesh location. The main gearbox lubrication system provided oil to the loading vanes using a high-pressure pump. Also, the main gearbox lubrication system provided oil to

the slave gears and support bearings. The test gear and main gearbox lubrication systems were separated by labyrinth seals on the gear shafts pressurized with nitrogen gas. Even though two separate systems existed, a common oil was used for both since some leakage occurred between the two. The lubricant used was a synthetic paraffin oil. In addition, the test gear lubricant was filtered through a 5-micron fiberglass filter.

The spur gear fatigue rig was primarily developed for surface pitting fatigue life investigations. For surface pitting fatigue tests, the test gears are run offset to increase the tooth contact stress and promote surface fatigue. For the current crack propagation studies, however, the desired failure mode was tooth bending fatigue. Therefore, the gears were run with full tooth width contact, not offset.

The test gear geometry data are given in Table I. The gears were external spur gears. The teeth had involute profiles with linear tip relief starting at the HPSTC and ending at the tooth tip. The maximum amount of tip relief was 0.013 mm at the tooth tip. The test gear material was consumable-electrode vacuum-melted AISI 9310 steel. The gears were case-carburized and ground. The teeth were hardened to a case hardness of R_c 61 and a core hardness of R_c 38. The effective case depth (depth at a hardness of R_c 50) was 0.81 mm. Previous studies on these test gears showed that speed effects on crack propagation direction would be most prevalent for a backup ratio of m_b=0.5 [7]. Thus, slots were machined in the gears to give a backup ratio of m_b=0.5 (Fig. 5a).

Table I. Test gear geometry
(gear tolerance per AGMA class 12)

Number of teeth	28
Module, mm	3.175
Whole depth, mm	7.620
Addendum, mm	3.175
Base circle radius, mm	41.77
Chordal tooth thickness, mm	4.851
Pressure angle, deg	20
Pitch diameter, mm	88.90
Outside diameter, mm	95.25
Root fillet, mm	1.016 to 1.524
Tip relief (at tooth tip), mm	0.013
Tooth profile surface finish, μm rms	0.41
Tooth and rim width, mm	6.35
Hub width, mm	19.05

It was believed that tooth bending fatigue cracks would be difficult to initiate based on the load capacity of the test rig. Due to this limitation, notches were fabricated in the fillet region (loaded side) on one tooth of each of the test gears to promote crack initiation. Notch specifications were as follows: 0.25 to 0.50-mm notch length, 40.5-mm notch mouth radius (location of greatest tensile stress of an uncracked gear), notch angle normal to fillet surface, notch machined along entire tooth face width. Fig. 5b shows a magnified view of a typical notched tooth. The notches were fabricated using electrodischarge machining (EDM) with a 0.10-mm diameter wire electrode. A total of four test gears had notches installed. Table II gives the measured notch characteristics. Fig. 6 gives the nomenclature for the notch parameters of Table II.

The objective of the tests was to determine the effect of speed on gear crack propagation direction. Four tests were performed. Test 1 was run at 2500 rpm, test 2 at 4920 rpm, test 3 at 7500 rpm, and test 4 at 10,000 rpm (Table II). Note that test 2 was originally specified for 5000 rpm, but was reduced to 4920 rpm due to facility resonance conditions. At the start of each test, the gears were run for a short break-in period of 20 to 123 N·m torque. After break-in, the gears were run at a steady load condition of 123 N·m. If fracture did not occur after a reasonable period of time, the load was

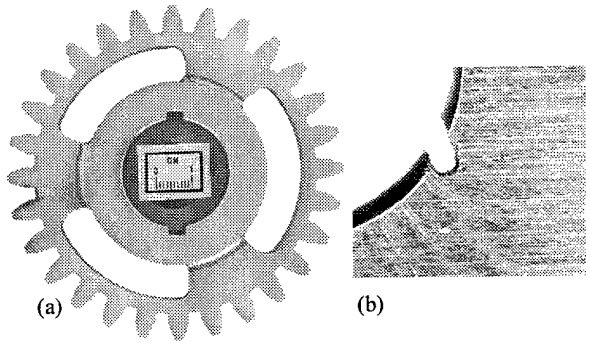

Fig. 5. Test gear, m_B=0.5. (a) full view, (b) magnified view of notch in tooth fillet.

Table II. Measured notch characteristics.

Test (test gear)	Notch mouth, R_0 (mm)	Notch length, l (mm)	Notch angle, γ (deg)	Test speed (rpm)
1	40.50	0.36	93.8	2500
2	40.60	0.32	108.7	4920
3	40.42	0.50	96.3	7500
4	40.50	0.26	118.5	10,000

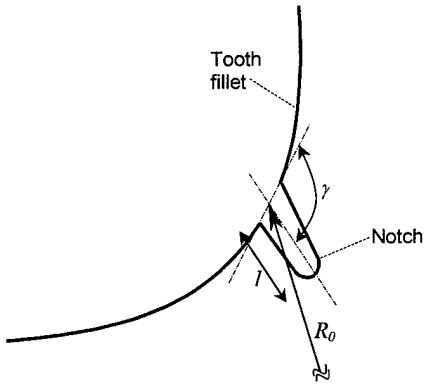

Fig. 6. Measured notch characteristics nomenclature .

incrementally increased and the gear were run until fracture occurred. The actual run loads ranged from 123 to 152 N·m. Test gear oil inlet temperature was set at 46° C. After occurrence of a failure (tooth or rim breakage), the gears were removed from the rig, cleaned, and photographed.

RESULTS AND DISCUSSION

Rotating Disk Model

Before analyzing gears, the FRANC finite element solution using the body force loading option was compared to a closed-form theoretical solution of a rotating disk. This was done to validate the solution using the body force load option of the program. A thin disk of uniform thickness rotating with a constant angular velocity ω was considered. The finite element model of the disk is shown in Fig. 7a. The inner and outer radii of the disk were a=14.73 mm and b=48.26 mm, respectively. The disk thickness was 25.40 mm. These dimensions roughly matched those of the test gears used in the study. However, no slots were used such as with the test gears. Material properties for steel were used (Young's modulus: E=207 GPa, Poisson's ratio: ν=0.3, mass density: ρ=7700 kg/m^3). The model had 768 8-node, plane stress, quadrilateral elements and 2432 nodes. Only body force due to the angular velocity was used

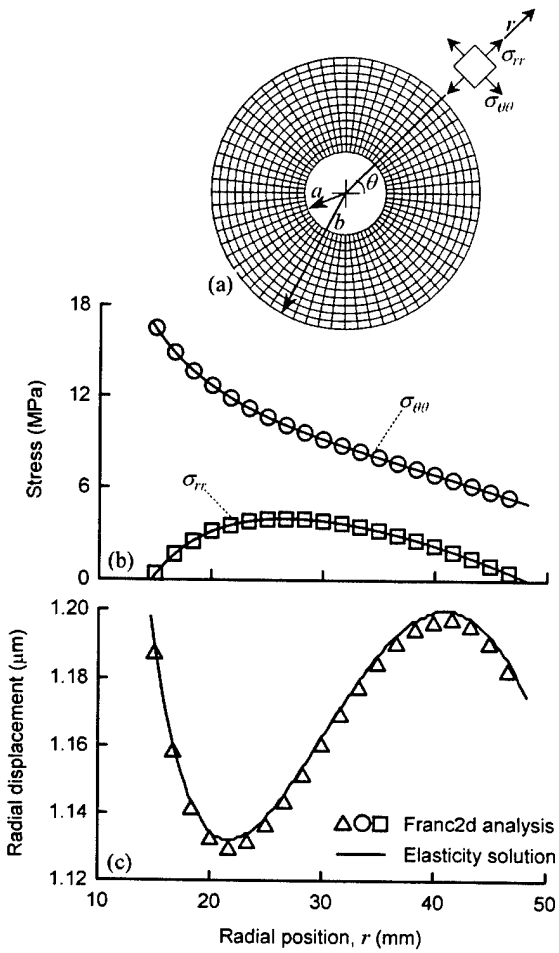

Fig. 7. Comparison of finite element analysis to closed-form elasticity solution for a rotating disk. (a) finite element model, (b) stresses, (c) displacements.

as applied loading. Four nodes of the inner radius were fixed to prevent rigid body motion but allow the disk to grow radially. The stresses and displacements from the finite element analysis are shown in Fig. 7b and 7c for an angular velocity of ω=1047.2 rad/s. These compared rather well to those calculated from the closed-form elasticity solution of [17].

Comparison of Predicted and Experimental Gear Crack Paths

The results of the crack propagation experiments performed in the gear fatigue rig are shown in Fig. 8. As stated before, four experiments were performed. Test 1 was run at 2500 rpm (Fig. 8a), test 2 at 4920 rpm (Fig. 8b), test 3 at 7500 rpm (Fig. 8c), and test 4 at 10,000 rpm (Fig. 8d). Again, the measured notch dimensions of the four test gears are shown in Table II. From the experiments, all cracks originated from the notch tip. For tests from 2500 to 7500 rpm, tooth fractures occurred. For the test at 10,000 rpm, rim fracture occurred. For the test at 2500 rpm, tooth fracture occurred at an applied torque of 152 N·m. For all other tests, fracture occurred at an applied torque of 123 N·m.

The predicted crack paths from the finite element analysis are compared to the actual crack paths from the experiments in Fig. 8. Separate finite element models were analyzed for each test gear configuration. Again, the models incorporated slots to give a backup ratio of m_b=0.5. Initial cracks were inserted in the models to correlate with the corresponding notch size, location, and orientation of the test gears from Table II. Tooth loads were placed at the HPSTC and the magnitudes corresponded to the applied

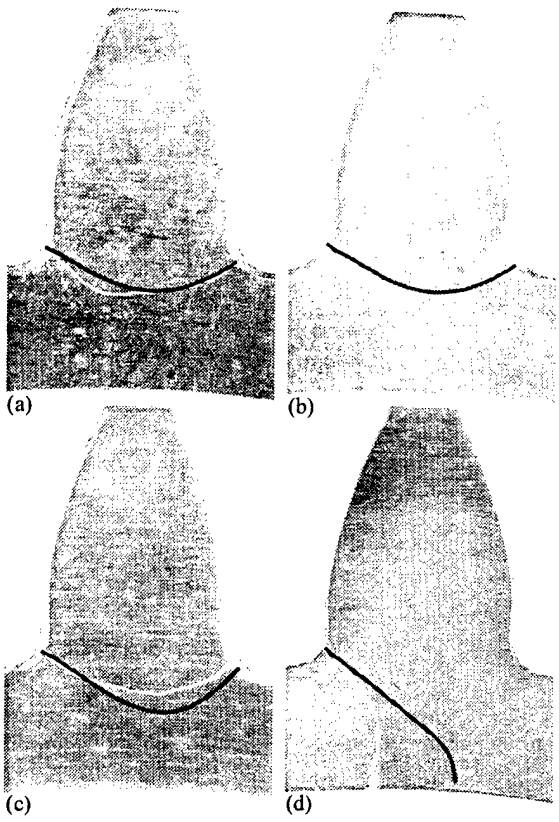

Fig. 8. Comparison of predicted crack paths with experiments (black lines: predictions, white lines: experiments). (a) 2500 rpm, (b) 4920 rpm, (c) 7500 rpm, (d) 10000 rpm.

torque at fracture of the given test. Also, body loads were applied corresponding to the gear speed of the given test. Crack propagation was numerically simulated using a crack increment size of 0.25 mm. This took 24 to 27 steps to reach the tooth or rim boundaries. For models at speeds of 2500 to 7500 rpm, tooth fracture occurred. For the model at 10,000 rpm, rim fracture occurred. This correlated very nicely with the experiments (Fig. 8).

Further analysis was performed on the finite element models described above. Each of the models of the test gears in Fig. 8 were analyzed at gear speeds of 2500, 5000, 7000, and 10,000 rpm. For the models of Figs. 8a (test gear 1) and 8b (test gear 2), tooth fractures were predicted for all speeds. For the models of Figs. 8c (test gear 3) and 8d (test gear 4), rim fractures were predicted at a speed of 10,000 rpm and tooth fractures were predicted at all other speeds. For the model of test gear 3, the notch mouth radius was slightly lower than the other cases (Table II, test gear 3, 7500 rpm). For the model of test gear 4, the notch orientation angle was slightly larger than the other cases (Table II, test gear 4, 10,000 rpm). These later two conditions tended to start the initial crack more toward the tooth root, and thus, promoted rim fractures at the higher speeds.

It should also be noted that the effect of speed on predicted crack path is dependent on the magnitude of the applied tooth load as well as the magnitude of the gear speed. This is due to the fact that the crack propagation angle is a function of K_{II} / K_I, and the stress intensity factors are determined from the superposition of the applied tooth load and body force. Crack propagation paths due to only the applied tooth load can lead to tooth or rim fracture, depending on the tooth design, backup ratio, and location of the initial crack. Crack propagation paths due to the speed-related body force lead to rim fracture due to the hoop stress component. Thus, the crack path due to the superposition of the tooth load and body load is dependent on the relative contributions due to each.

As an example of this, the model of the test gear in Fig. 8c at 7500 rpm and 123 N·m torque predicted tooth fracture while the same model at 7500 rpm and 61 N·m predicted rim fracture.

Parametric Studies

Parametric studies were performed using the FRANC finite element crack propagation code. The effects of speed, backup ratio, and initial crack location on gear crack propagation direction were investigated. Backup ratios of m_b=0.3, 0.5, 0.7, 1.0, and 1.3 were studied. Gear speeds of 0, 5000, 10,000, and 15,000 rpm were used. Initial crack locations from those slightly below the base circle on the tooth fillet to those on the tooth root centerline were investigated. For all cases, the applied tooth load was placed at the HPSTC and corresponded to an applied torque of 123 N·m.

Fig. 9 shows the analysis for a backup ratio of m_b=0.3. For an initial crack mouth location of R_0=41.33 mm (slightly below the base circle), rim fracture occurred for a speed of 15,000 rpm and tooth fracture occurred for all other speeds (Fig. 9a). For initial cracks mouth locations lower than R_0=41.33 mm, rim fractures occurred for all speeds (R_0=40.81 mm shown in Fig. 9b). Fig. 10 shows the analysis for a backup ratio of m_b=0.5. Here, the transition point was at R_0=40.35 mm. At R_0=40.35 mm, tooth fractures occurred for 0 and 5000 rpm while rim fractures occurred at 10,000 and 15,000 rpm (Fig. 10b). For R_0>40.35 mm, tooth fractures occurred for all speeds (Fig. 10a). For R_0<40.35 mm, rim fractures occurred for all speeds (Fig. 10c). Fig. 11 shows the analysis for a backup ratio of m_b=0.7. Here, the tooth/rim fracture transition point was at R_0=41.33 mm. Fig. 12 shows the analysis for a backup ratio of m_b=1.0 and Fig. 13 shows the analysis for a backup ratio of m_b=1.3. For both of these cases, the tooth/rim fracture transition point was at the root centerline.

As seen from these studies, speed had little effect on crack propagation direction except when the initial crack location was near the tooth/rim fracture transition point for the given backup ratio. When at that point, higher speeds tended to promote rim fracture while lower speeds (or neglecting centrifugal force) produced tooth fractures.

CONCLUSIONS

The effect of speed (centrifugal force) on gear crack propagation direction was explored. Gears were analyzed using finite element analysis and linear elastic fracture mechanics. The analysis was validated from crack propagation experiments performed in a spur gear fatigue rig. The effects of speed, backup ratio, and initial crack location on gear crack propagation direction were investigated. The following conclusions were derived:

1) Stresses and deflections from the finite element method correlated well with a closed-form elasticity solution for a rotating disk example problem. Crack paths from the finite element method correlated well with those deduced from gear experiments.

2) For the test gear with a backup ratio of m_b=0.5, cracks initiating in the tooth fillet propagated to rim fractures when run at a speed of 10,000 rpm and tooth fractures for speeds slower than 10,000 rpm for both the experiments and analysis.

3) Speed had little effect on crack propagation direction except when initial crack locations were near the tooth/rim fracture transition point for a given backup ratio. When at that point, higher speeds tended to promote rim fracture while lower speeds (or neglecting centrifugal force) produced tooth fractures.

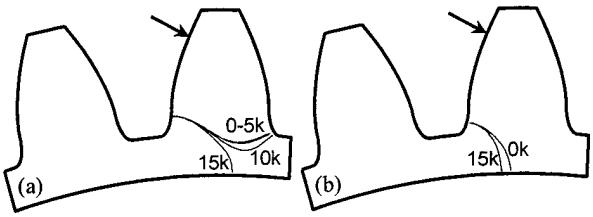

Fig. 9. Effect of speed on crack propagation path, m_B=0.3. (a) R_0=41.33 mm, (b) R_0=40.81 mm.

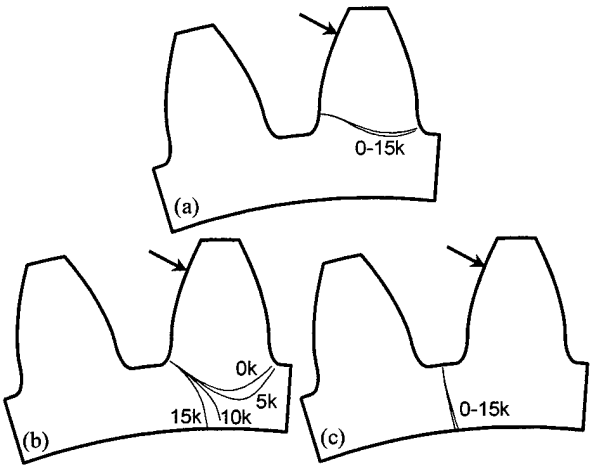

Fig. 10. Effect of speed on crack propagation path, m_B=0.5. (a) R_0=41.33 mm, (b) R_0=40.35 mm, (c) R_0=root centerline.

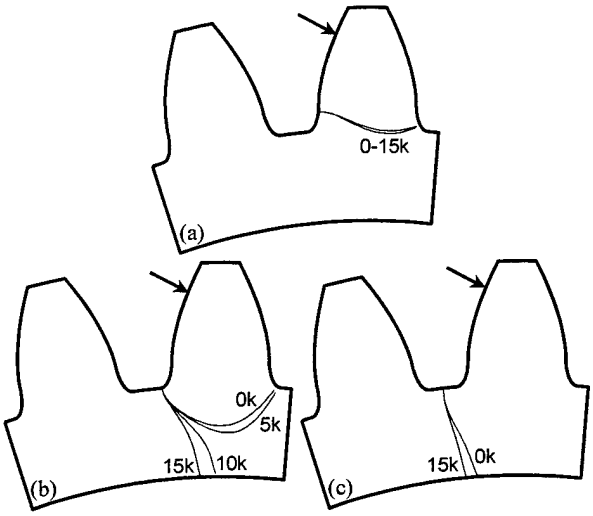

Fig. 11. Effect of speed on crack propagation path, m_B=0.7. (a) R_0=41.33 mm, (b) R_0=40.03 mm, (c) R_0=root centerline.

REFERENCES

1. Couchan, D.C., Barnes, G.K., and Cedoz, R.W., "Shot-Peened Gear Failures Due to Operation in a Misaligned Condition", AIAA Paper No. AIAA-93-2147 (1993).
2. Albrecht, C., "Transmission Design Using Finite Element Method Analysis Techniques", *Journal of American Helicopter Society*, Vol. 33, No. 2 (1988), 3-14.
3. Abersek, B., and Flasker, J., "Stress Intensity Factor for Cracked Gear Tooth", *Theoretical and Applied Fracture Mechanics*, Vol. 20, No. 2 (1994), 99-104.
4. Sfakiotakis, V.G., Katsareas, D.E., and Anifantis, N.K., "Boundary Element Analysis of Gear Teeth Fracture", *Engineering Analysis with Boundary Elements*, Vol. 20, No. 2 (1997), 169-175.
5. Arikin, M.A., Tarhan, A.I., and Yahoj, O.S., "Life Estimate of a Spur Gear with a Tooth Cracked at Fillet Region", *Proceedings of the ASME Design Engineering Technical Conference*, Atlanta, GA, USA (1998).
6. Abersek, B., and Flasker, J., "Experimental Analysis of Propagation of Fatigue Crack on Gears", *Experimental Mechanics*, Vol. 38, No. 3 (1998), 226-230.
7. Lewicki, D.G., and Ballarini, R., "Effect of Rim Thickness on Gear Crack Propagation Path", *Journal of Mechanical Design*, Vol. 119, No. 1 (1997), 88-95.
8. Ciavarella, M., and Demelio, G., "Numerical Methods for the Optimization of Specific Sliding, Stress Concentration, and Fatigue Life of Gears", *International Journal of Fatigue*, Vol. 21, No. 5 (1999), 465-474.
9. Lewicki, D.G., Spievak, L.E., Wawrzynek, P.A., Ingraffea, A.R., and Handschuh, R.F., "Consideration of Moving Tooth Load in Gear Crack Propagation Predictions", *Proceedings of the 8th International Power Transmission and Gearing Conference*, Baltimore, MD, USA (2000).
10. Spievak, L.E., Wawrzynek, P.A., Ingraffea, A.R., and Lewicki, D.G., "Simulating Fatigue Crack Growth in Spiral Bevel Gears", *Engineering Fracture Mechanics*, Vol. 68, No. 1 (2001), 53-76.
11. Wawrzynek, P.A., Carter, B.J., and Ingraffea, A.R., "Life Prediction of Turbine Blades by Computer Modeling", SBIR Phase II Final Report, Contract No. N688335-94-C-0193 (1998).
12. Hefeng, B., Savage, M., and Knorr, R.J., "Computer Modeling of Rack-Generated Spur Gears", *Mechanism and Machine Theory*, Vol. 20, No. 4 (1985), 351-360.
13. P3/PATRAN, P3/PATRAN User Manual, PDA Engineering, Costa Mesa, CA, USA (1993).
14. Wawrzynek, P.A., "Discrete Modeling of Crack Propagation: Theoretical Aspects and Implementation Issues in Two and Three Dimensions", Ph.D. Dissertation, Cornell University (1991).
15. Rice, J.R., "A Path Independent Integral and the Approximate Analysis of Strain Concentration by Notches and Cracks", *Journal of Applied Mechanics*, Vol. 35 (1968), 379-386.
16. Erdogan, F., and Sih, G.C., "On the Crack Extension in Plates Under Plane Loading and Transverse Shear", *Journal of Basic Engineering*, Vol. 85 (1963), 519-527.
17. Saada, A.S., Elasticity, Theory and Applications, First Edition, *Kreiger Publishing* (1983), 334-337.

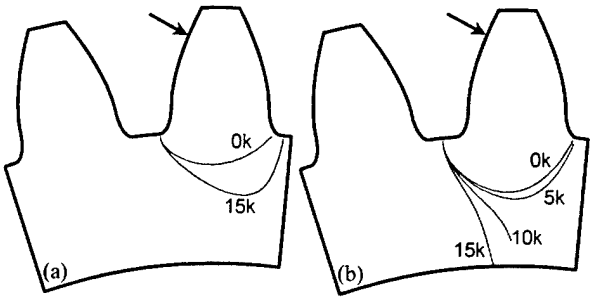

Fig. 12. Effect of speed on crack propagation path, m_B=1.0. (a) R_0=40.01 mm, (b) R_0=root centerline.

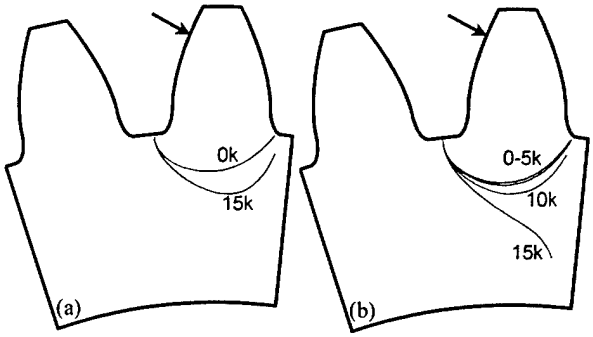

Fig. 13. Effect of speed on crack propagation path, m_B=1.3. (a) R_0=39.99 mm, (b) R_0=root centerline.

REPORT DOCUMENTATION PAGE

Form Approved
OMB No. 0704-0188

1. AGENCY USE ONLY (*Leave blank*)	2. REPORT DATE	3. REPORT TYPE AND DATES COVERED
	August 2001	Technical Memorandum

4. TITLE AND SUBTITLE

Effect of Speed (Centrifugal Load) on Gear Crack Propagation Direction

5. FUNDING NUMBERS

WU–712–30–13-00
1L162211A47A

6. AUTHOR(S)

David G. Lewicki

7. PERFORMING ORGANIZATION NAME(S) AND ADDRESS(ES)

National Aeronautics and Space Administration
John H. Glenn Research Center
Cleveland, Ohio 44135–3191
and
U.S. Army Research Laboratory
Cleveland, Ohio 44135–3191

8. PERFORMING ORGANIZATION REPORT NUMBER

E–12963

9. SPONSORING/MONITORING AGENCY NAME(S) AND ADDRESS(ES)

National Aeronautics and Space Administration
Washington, DC 20546–0001
and
U.S. Army Research Laboratory
Adelphi, Maryland 20783–1145

10. SPONSORING/MONITORING AGENCY REPORT NUMBER

NASA TM—2001-211117
ARL–TR–1314

11. SUPPLEMENTARY NOTES

Prepared for the International Conference on Motion and Power Transmissions sponsored by the Japan Society of Mechanical Engineers, Fukuoka, Japan, November 15–17, 2001. Responsible person, David G. Lewicki, organization code 5950, 216–433–3970.

12a. DISTRIBUTION/AVAILABILITY STATEMENT

Unclassified - Unlimited
Subject Category: 37 Distribution: Nonstandard

Available electronically at http://gltrs.grc.nasa.gov/GLTRS

This publication is available from the NASA Center for AeroSpace Information, 301–621–0390.

12b. DISTRIBUTION CODE

13. ABSTRACT ***(Maximum 200 words)***

The effect of rotational speed (centrifugal force) on gear crack propagation direction was explored. Gears were analyzed using finite element analysis and linear elastic fracture mechanics. The analysis was validated with crack propagation experiments performed in a spur gear fatigue rig. The effects of speed, rim thickness, and initial crack location on gear crack propagation direction were investigated. Crack paths from the finite element method correlated well with those deduced from gear experiments. For the test gear with a backup ratio (rim thickness divided by tooth height) of $m_b = 0.5$, cracks initiating in the tooth fillet propagated to rim fractures when run at a speed of 10,000 rpm and became tooth fractures for speeds slower than 10,000 rpm for both the experiments and analysis. From additional analysis, speed had little effect on crack propagation direction except when initial crack locations were near the tooth/rim fracture transition point for a given backup ratio. When at that point, higher speeds tended to promote rim fracture while lower speeds (or neglecting centrifugal force) produced tooth fractures.

14. SUBJECT TERMS

Gears; Crack propagation; Fracture mechanics; Finite element method; Centrifugal force

15. NUMBER OF PAGES

12

16. PRICE CODE

17. SECURITY CLASSIFICATION OF REPORT	18. SECURITY CLASSIFICATION OF THIS PAGE	19. SECURITY CLASSIFICATION OF ABSTRACT	20. LIMITATION OF ABSTRACT
Unclassified	Unclassified	Unclassified	